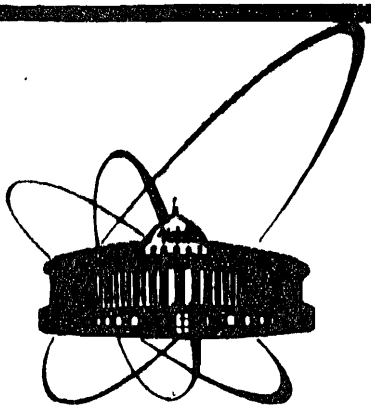

сообщения
объединенного
института
ядерных
исследований
дубна

E17-87-554

R.Taranko, E.Taranko, J.Malek

SELF-CONSISTENT TREATMENT OF COULOMB CORRELATIONS IN TRANSITION METALS

1987

1. INTRODUCTION

The electronic structure of metals may be investigated by means of many spectroscopic techniques (e.g. by X-ray emission and absorption, X-ray photoemission, UV photoemission, angle-resolvent photoemission spectroscopy, etc). Results of these experiments are usually compared with the one-electron band structure calculations. Now it is well known that for some metals the photoemission measurements show a disagreement between experimental and calculated d-bandwidth. For example, the width of the valence-band photoemission spectrum of nickel is by about 30% smaller than it is predicted by the band-structure calculations. Furthermore, in nickel, there is a satellite structure about 6 eV below the Fermi level in the experimental density of states[1]. This satellite structure has received much attention in literature[2-7]. Some authors[8] explain the resonant behaviour of the experimental 6 eV peak as a conventional intraband excitation effect arising from a large enhancement in the projected joint density of states. A more widely accepted point of view, however, is that the reduction in the bandwidth and the satellite structure can be shown to arise from many-body effects within the unfilled d-band. A convenient frame for a description of such processes is the degenerate Hubbard hamiltonian with a contact electron-electron interaction. The problem of electron correlations is usually treated in T-matrix approximation (TMA)[3,4] or using the second-order perturbation theory (SOPT) in U/W[7-19], where U is the strength of the contact Coulomb interaction and W denotes the one-electron bandwidth. The advantage of the SOPT approach is that it works for an arbitrary particle concentration whereas the TMA technique remains valid only for low particle concentrations. On the other hand, the SOPT treatment is limited to values of the U/W ratio smaller than 0.5.

All the above-mentioned SOPT calculations[7-19] have been however performed in a non-self-consistent way. Therefore, the self-energy calculated in such a manner at T = 0°K vanishes at the one-electron Fermi energy E_F^0 instead of quasiparticle (many-body) Fermi energy E_F, causing the quasiparticles

at energy $E_F - E_F^\circ$ below the true Fermi level to have infinite lifetimes and these on E_F to have short lifetimes[9]. For that reason, Kleinman and Mednick[9] had to make some energy shift (the value of which is not immediately transparent) to restore the proper behaviour of the imaginary part of the self-energy at the many-body Fermi level.

In this paper we report on self-consistent calculations of the density of states for quasiparticles described by the Hubbard hamiltonian. The organization of our paper is as follows. In Section 2 we give a short recapitulation of the SOPT approach developed by Treglia et al.[7] and describe the self-consistent procedure. In Section 3 we present some analytical results for the self-energy we have found to be useful in programming this or related problems at computers. In Section 4 we give a comparison of the one-particle spectrum and the spectral densities of states for the single and degenerate band Hubbard hamiltonian calculated in a self-consistent and non-self-consistent way. Finally, in Appendix, one can find analytical formulas for the self-energy arising from the rectangular uncorrelated density of states.

2. THEORY

Let us start with the degenerate Hubbard hamiltonian for a d-band:

$$H = H_0 + \frac{U}{2} \sum_{i\nu\nu'\sigma\sigma'} (1 - \delta_{\nu\nu'}\delta_{\sigma\sigma'}) n_{i\nu\sigma}\, n_{i\nu'\sigma'}, \tag{1}$$

where H_0 is the band hamiltonian; U is the average on-site Coulomb interaction, the same for each of the five d-bands (label ν); σ denotes a spin index and $n_{i\nu\sigma}$ is the particle-number operator. The self-energy written in the first and second order in U/W reads as[7] (the spin index σ will be suppressed as we are dealing with the paramagnetic case):

$$\Sigma(\vec{k},E) = \frac{9}{10} U N_e + 9U^2 \sum_{\vec{p}\,\vec{q}} \frac{f_{\vec{p}+\vec{q}}(1-f_{\vec{q}})(1-f_{\vec{k}+\vec{p}}) + (1-f_{\vec{p}+\vec{q}})\, f_{\vec{q}}\, f_{\vec{k}+\vec{p}}}{E^+ + \epsilon(\vec{p}+\vec{q}) - \epsilon(\vec{k}+\vec{p}) - \epsilon(\vec{q})}, \tag{2}$$

where $f_{\vec{k}}$ is the Fermi distribution function for the state $|\vec{k}\rangle$ of the energy $\epsilon(\vec{k})$; the N_e denotes the number of electrons per atom and the indices $\vec{p}, \vec{q}$ run over the first B.Z. of the crystal. It is convenient to subtract from the self-energy its Hartree-Fock part (the first term of Eq. (2)) and to rewrite its second-order part in U/W (the second term of Eq. (2)) as

$$M(\vec{k},E) = 9U^2 \sum_{\vec{R}} e^{i\vec{k}\cdot\vec{R}} \iiint_{-\infty}^{+\infty} \frac{d\omega_1 d\omega_2 d\omega_3}{E^+ + \omega_1 - \omega_2 - \omega_3} \times$$
$$\times N(\omega_1,\omega_2,\omega_3) D_{\vec{R}}(\omega_1) D_{\vec{R}}(\omega_2) D_{\vec{R}}(\omega_3), \tag{3}$$

where

$$D_{\vec{R}}(\omega) = \frac{1}{N} \sum_{\vec{k}} e^{i\vec{k}\cdot\vec{R}}\, \delta(\omega - \epsilon(\vec{k})). \tag{4}$$

The function $N(\omega_1,\omega_2,\omega_3)$ combines all $f_{\vec{k}}$ factors appearing in Eq. (2) and $\vec{R}$ denotes atomic positions in the crystal. The local approximation for the self-energy introduced by Treglia et al.[7] corresponds to retaining of the first term ($\vec{R} = 0$) in Eq. (3) only; so we have

$$M(\vec{k},E) \Rightarrow M(E) = 9U^2 \iiint_{-\infty}^{+\infty} \frac{d\omega_1 d\omega_2 d\omega_3}{E^+ + \omega_1 - \omega_2 - \omega_3} \times$$
$$\times N(\omega_1,\omega_2,\omega_3) D(\omega_1) D(\omega_2) D(\omega_3), \tag{5}$$

where $D(\omega) \equiv D_{\vec{R}=0}(\omega)$ is the local density of states (LDOS) corresponding to the band structure $\epsilon(\vec{k})$ (see Eq. (4)). The main merit of the local approximation lies in the fact that the self-energy obtained through Eq. (5) is $\vec{k}$-independent and directly connected to LDOS.

Now we are in good position to describe a self-consistent procedure for a calculation of the quasiparticle density of states. At first, let us recall that the one-particle spectral density of states is given by the imaginary part of the perturbed retarded Green function:

$$G(\vec{k},E) = (E^+ - \epsilon(\vec{k}) - \Sigma(\vec{k},E))^{-1} \tag{6}$$

and the quasiparticle LDOS (very often called the one-particle spectrum) is obtained by summing the imaginary part of Eq. (6) over wave vector $\vec{k}$:

$$D(E) = -\frac{1}{\pi} \mathrm{Im} \frac{1}{N} \sum_{\vec{k}} G(\vec{k},E) \cong$$
$$\cong -\frac{1}{\pi} \mathrm{Im} \int_{-\infty}^{+\infty} \frac{D_0(\eta)}{E^+ - \Sigma(E) - \eta} d\eta = -\frac{1}{\pi} \mathrm{Im} \int_{-\infty}^{+\infty} \frac{D_0(\eta - 9U\nu)}{E^+ - M(E) - \eta} d\eta, \tag{7}$$

where $\nu = N_e/10$ is the band filling and $D_0(\eta)$ is the local density of states corresponding to uncorrelated band structure $\epsilon(\vec{k})$. If μ is the chemical potential of the quasiparticles, then at the absolute zero of temperature we have $(\mu = E_F)$

$$\nu = \int_{-\infty}^{E_F} D(E)\, dE , \tag{8}$$

where the quasiparticle Fermi energy E_F may differ from the one-electron Fermi level E_F° found in the Hartree-Fock solution of the Hubbard hamiltonian. To find $D(E)$ and E_F in a self-consistent way we start with the one-electron density of states per atom $D_0(E)$ and calculate the second-order part of the self-energy $M(E)$ from Eq. (5). Then, the quasiparticle LDOS (one-particle spectrum) and Fermi level E_F are found from Eqs. (7) and (8) and used as input data for an iteration process carried out by Eqs. (5), (7) and (8). Let us note that at each iteration step the imaginary part of the self-energy has the proper behaviour at Fermi level E_F, and therefore, no artificial energy shifts are needed. The iteration process is terminated when a desired accuracy of $D(E)$ and E_F is achieved (for numerical details see Section 4).

3. SELF-ENERGY

To carry out the self-consistent process efficiently, one needs a fast numerical procedure for the evaluation of the complex function $M(E)$ (see eq. (5)). From a numerical point of view the best way is at first to calculate the imaginary part of $M(E)$ and then to find the real part of $M(E)$ from the dispersion relation

$$\mathrm{Re}\, M(E) = -\frac{1}{\pi} \int_{-\infty}^{+\infty} \frac{\mathrm{Im}\, M(\eta)}{E-\eta} d\eta . \tag{9}$$

At temperature $T = 0^\circ K$ the imaginary part of $M(E)$ takes the form

$$\mathrm{Im}\, M(E) = -9\pi U^2 \iiint_{-\infty}^{+\infty} d\omega_1 d\omega_2 d\omega_3\, N(\omega_1,\omega_2,\omega_3) D(\omega_1) D(\omega_2) D(\omega_3) \times$$

$$\times \delta(E+\omega_1-\omega_2-\omega_3) = -9U^2\pi \Big\{ \int_a^{E_F} d\omega_1 \int_{E_F}^{b} d\omega_2 \int_{E_F}^{b} d\omega_3\, D(\omega_1) D(\omega_2) D(\omega_3) \times$$

$$\times \delta(E+\omega_1-\omega_2-\omega_3) + \int_{E_F}^{b} d\omega_1 \int_a^{E_F} d\omega_2 \int_a^{E_F} d\omega_3\, D(\omega_1) D(\omega_2) D(\omega_3) \times$$

$$\times \delta(E+\omega_1-\omega_2-\omega_3) \Big\} \equiv -9\pi U^2 (S_1(E) + S_2(E)) ,$$

where a and b, respectively, are the lower and upper limits of the energy band $D(\omega)$. The function $S_1(E)$ equals zero for $E < E_F$ whereas $S_2(E) = 0$ for $E > E_F$. From the definition of $N(\omega_1, \omega_2, \omega_3)$ it follows that $\mathrm{Im}\, M(E_F) = 0$. It is also convenient to express the function $S_1(E)$ (and similarly $S_2(E)$) as

$$S_1(E) = \int_a^{E_F} d\omega_1 \int_{E_F}^{b} d\omega_2 D(\omega_1) D(\omega_2) D(E+\omega_1-\omega_2)\, \theta(b-E-\omega_1+\omega_2) \times$$

$$\times \theta(E+\omega_1-\omega_2-E_F) = \int_a^{E_F} d\omega_1 \int_{\omega_1-b}^{\omega_1-E_F} d\omega_2 D(\omega_1) D(\omega_1-\omega_2) D(E+\omega_2) \times \tag{11}$$

$$\times \theta(E+\omega_2-E_F) \cdot \theta(b-E-\omega_2) ,$$

where

$$\theta(x) = \begin{cases} 1 & \text{for } x \geq 0 \\ 0 & \text{for } x < 0. \end{cases} \tag{12}$$

From the definition of $\theta(x)$ it follows that the integrand in Eq. (11) is nonzero only for $b - E \geq \omega_2 \geq E_F - E$. A typical shape of an integration region is displayed in Figs. 1 and 2.

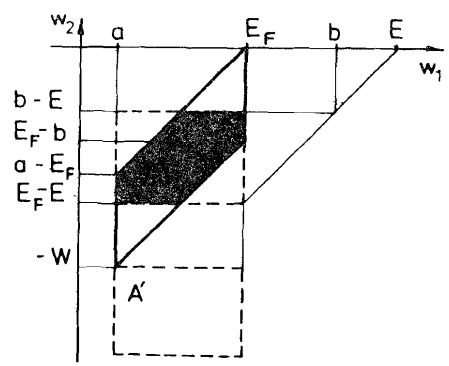

Fig. 1. The 2D-integration area for numerical evaluation of the function $S_1(E)$ defined by Eq. (11); $E > E_F$ and $E_F > a + W/2$ (see also text).

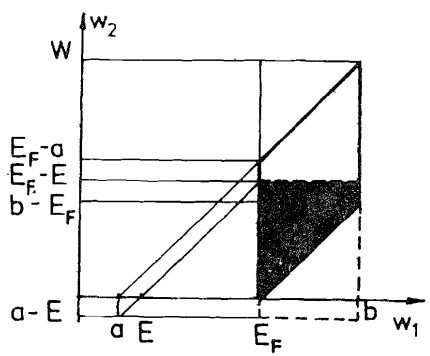

Fig. 2. The same as in Fig. 1 but for the function $S_2(E)$; $E < E_F$ and $E_F > a + W/2$.

The parallelogram B (full line) is fixed in the plane of variables (ω_1, ω_2) whereas the rectangle A (dashed line) moves

along the ω_2-axis in dependence of the energy E. The 2D-integration area is given by the overlap of the rectangle A and the parallelogram B.

The density of states for realistic d-band is very often [7,10] approximated by a rectangular density of states with a width W fitted to band calculation data. In this case, we have (the spin index σ is suppressed as we are dealing with the paramagnetic state; also, we work with an energy unit equal to half a bandwidth)

$$D_0(E) = \begin{cases} 1/2 & \text{for } |E| \leq 1 \\ 0 & \text{for } |E| > 1 \end{cases} \tag{13}$$

and, of course, the functions $S_1(E)$ and $S_2(E)$ may be calculated analytically. For example, when level E_F lies at the centre of the band ($E_F = 0$), one can easily find

$$\mathrm{Im}\, M(E) = -\frac{9\pi U^2}{8} S(E) , \tag{14a}$$

where

$$\begin{aligned} S(E) &= 0 && \text{for } E \leq -3 \\ &= \frac{1}{2}(E+3)^2 && \text{for } -3 \leq E \leq -2 \\ &= -E^2 - 3E - 1 && \text{for } -2 \leq E \leq -1 \\ &= \frac{1}{2} E^2 && \text{for } -1 \leq E \leq 1 \\ &= -E^2 + 3E - 1 && \text{for } 1 \leq E \leq 2 \\ &= \frac{1}{2}(3-E)^2 && \text{for } 2 \leq E \leq 3 \\ &= 0 && \text{for } 3 \leq E. \end{aligned} \tag{14b}$$

The corresponding real part of M(E) obtained from Eq.(3) reads

$$\mathrm{Re}\, M(E) = \frac{9U^2}{8} F(E) , \tag{15a}$$

where

$$\begin{aligned} F(x) = \frac{1}{2}\{&(3+x)^2 \ln|3+x| + (3-x)^2 \ln|3-x| + 3(2-x)^2 \ln|2-x| - \\ &- 3(2+x)^2 \ln|2+x| + 3(1+x)^2 \ln|1+x| - 3(1-x)^2 \ln|1-x|\}. \end{aligned} \tag{15b}$$

Let us note that for the rectangular $D_0(E)$ the function M(E)

can be found directly from Eq. (5) without using any dispersion relation. The relevant formulas for an arbitrary filling of the band are given in Appendix and they may be used for a discussion of the non-self-consistent results. The self-consistent procedure, however, can be carried out in the numerical way only (even for a starting rectangular LDOS). Hence, the knowledge of the analytical formulas helps us to debug appropriate numerical procedures.

4. NUMERICAL RESULTS AND DISCUSSION

We have numerically solved equations (5),(7) and (8) for the paramagnetic state. We have used a discrete energy mesh with the step equal to 0.05 times half a bandwidth W/2 and $0.01 \times W/2$, respectively. The step $0.05 \times W/2$ has appeared quite reasonable because more fine division of the energy scale has brought no significant effects. During the iteration process we have checked variations in the value of Fermi level $\epsilon_1^{(i)} = |E_F^{(i)} - E_F^{(i-1)}|$, Eq.(8), and in the shape of D(E), Eq.(7),

$$\epsilon_2^{(i)} = \frac{1}{M}\left(\sum_{\alpha=1}^{M} (D^{(i)}(E_\alpha) - D^{(i-1)}(E_\alpha))^2\right)^{1/2} , \tag{16}$$

where the index i counts the iterations and M is the number of points of the energy mesh lying within the band limits of D(E). To terminate the iteration process we have used the conditions $\epsilon_1^{(i)} \leq$ step of the energy mesh and $\epsilon_2^{(i)} \leq 10^{-4}$, where i is the number of the iteration step. The self-consistency has been achieved after 5-12 iterations.

Since equations (5) and (7) derived for the single band and the degenerate Hubbard hamiltonian, respectively, differ in multiplicative factor 9 only, one can study both the hamiltonians using the same numerical procedures. The calculated one-particle spectra are displayed in Figs. 3-9, where the lower part of the Figure corresponds to the non-self-consistent one-particle spectrum and the upper part to the self-consistent one. The origin of the energy scale is always set to the Fermi level and one half of the uncorrelated bandwidth W/2 is used as an energy unit. Furthermore, for each studied case (the rectangular or fcc uncorrelated LDOS) the value of U/W has been set to 0.5 and 0.25, respectively; so we have been able to estimate an influence of the strength of Coulomb correlations on a shape of LDOS.

At first, let us start to discuss the results obtained for the single-band Hubbard hamiltonian. The self-consistent cal-

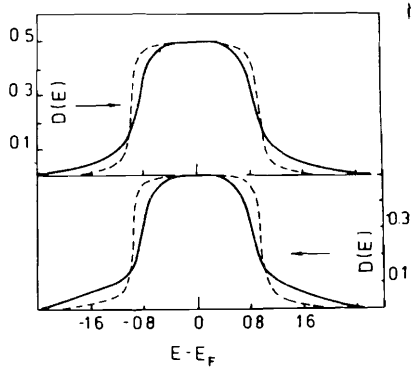

Fig.3. The one-particle spectrum for the single band Hubbard hamiltonian calculated for the rectangular $D_0(E)$. *The band filling is 0.5;* $U/W = 0.5$ *(full line) and* $U/W = 0.25$ *(dashed line). The lower and upper panel displays the non-self-consistent and self-consistent results, respectively. The half of the uncorrelated bandwidth* $W/2$ *is taken as an energy unit. The origin of the energy scale is set to the Fermi level.*

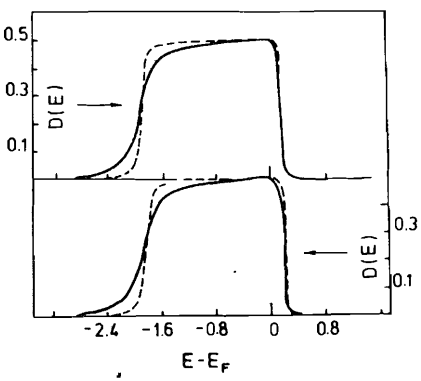

Fig.4. The same as in Fig.3 but for the band filling set to 0.9.

culations have been performed for the rectangular and for fcc starting local density of states $D_0(E)$. In both the cases the band filling has been set to 0.5 and 0.9, respectively. For the rectangular LDOS the band filling 0.5 gives rise to the symmetrical D(E) around the Fermi level (a useful property to test an accuracy of numerical procedures), whereas $\nu = 0.9$ roughly approximates the nickel value (the case investigated by many authors [7,9]). The results are shown in Figs. 3-6. One can immediately observe (Figs.3 and 4) that for the rectangular $D_0(E)$ the self-consistent process has no influence on the shape of D(E) regardless of the strength of Coulomb correlations. For the fcc starting LDOS the situation is slightly different. At the band filling 0.5 and the ratio $U/W = 0.5$ there is a peak at the right-hand side of the non-self-consistent one-particle spectrum (Fig.5) which disappears during the self-consistent process. At the band filling 0.9 (Fig.6) no additional structure appears at all regardless of a value of the ratio U/W. The one-particle spectra calculated for the degenerate Hubbard hamiltonian are displayed in Figs.7-9. In accord with calculations of Treglia et al.[7] for the rectangular $D_0(E)$ we have found two

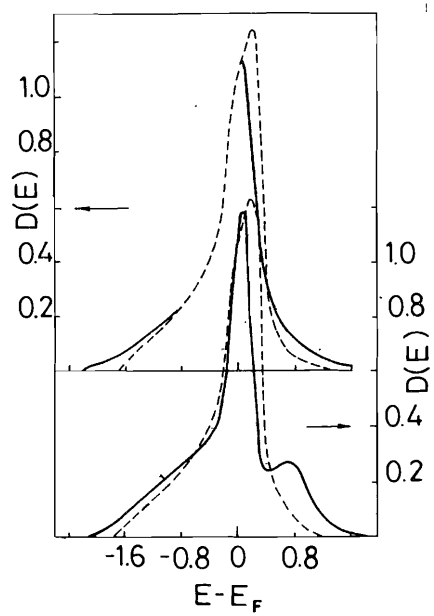

Fig.5. The same as in Fig.3 but for the case of the fcc uncorrelated LDOS. The band filling equals 0.5.

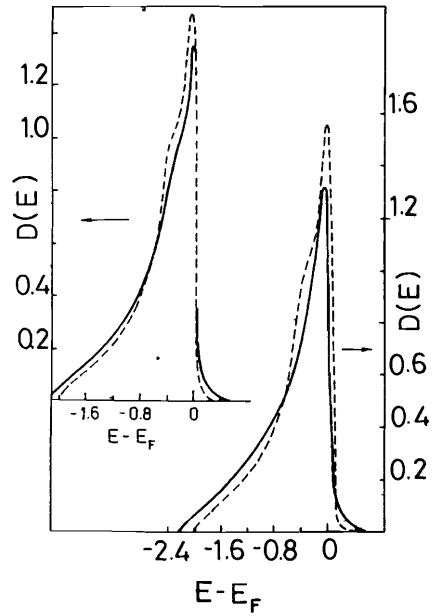

Fig.6. The same as in Fig.5 but the band filling is set to 0.9.

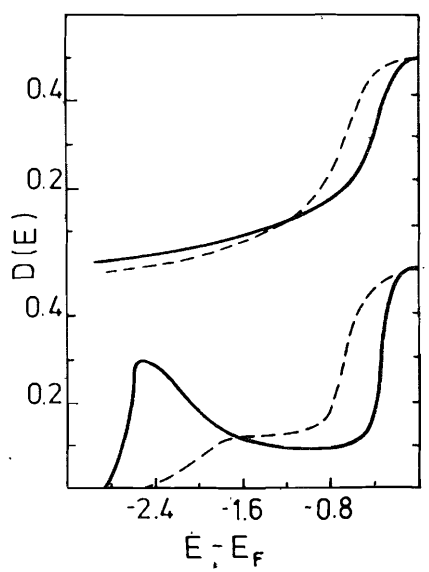

Fig.7. The one-particle spectrum for the degenerate Hubbard hamiltonian calculated for the rectangular $D_0(E)$. *The band filling is 0.5;* $U/W = 0.5$ *(full line) and 0.25 (dash line). For the symmetry reasons only the left-hand side of the spectrum is shown. See also the text in Fig. 3.*

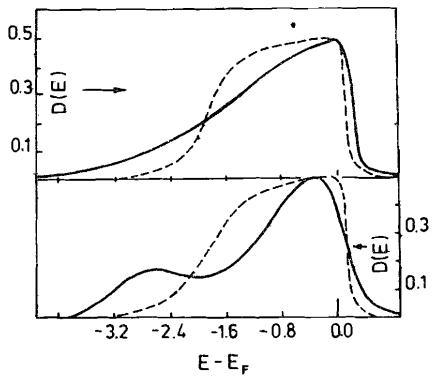

Fig.8. The same as Fig.7 but the band filling equals 0.9. The full spectrum is shown.

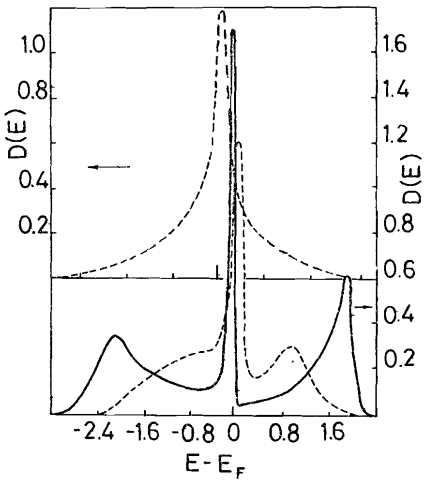

Fig.9. The same as in Fig.7 but for the case of the fcc *uncorrected* $D_0(E)$. *The full spectrum is displayed.*

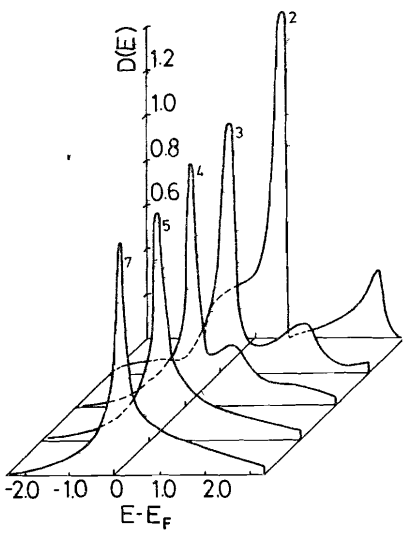

Fig.10. The fcc *one-particle spectrum for successive iterations steps (the upper index). The band filling is 0.5 and* $U/W = 0.25$.

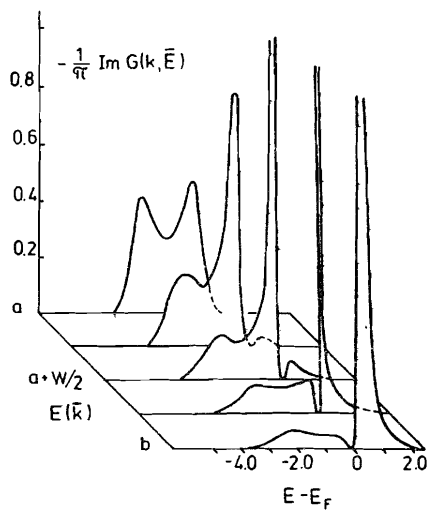

Fig.11. The non-self-consistent one-particle spectral density for the degenerate Hubbard hamiltonian calculated for the rectangular $D_0(E)$. *The band filling is 0.5 and* $U/W = 0.5$.

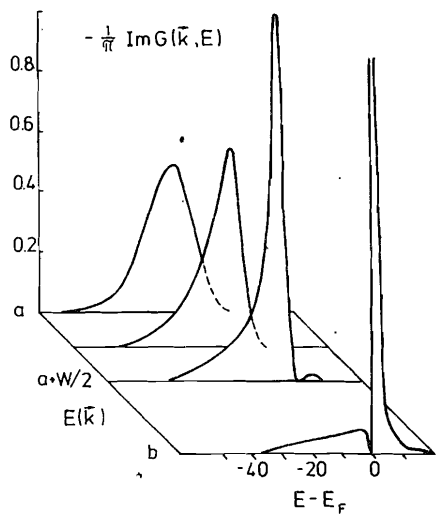

Fig.12. The same as in Fig.11 but calculated in a self-consistent way.

satellite peaks on the non-self-consistent one-particle spectrum which have however disappeared during the self-consistent process. Similarly, the self-consistent procedure removes any additional structure on the non-self-consistent fcc one-particle spectrum, too. This smoothing process is illustrated in Fig.10 where we show changes in the fcc $D^{(i)}(E)$ during successive iteraction steps. Finally, in Figs.11 and 12, one can compare one-particle spectral densities calculated in a non-self-consistent and a self-consistent way for the rectangular $D_0(E)$ using different values of $\epsilon(\bar{k})$. The non-self-consistent spectral densities (Fig.11) agree well with the results of Ref.[7] whereas Fig.12 once again demonstrates the smoothing properies of the self-consistent procedure.

SUMMARY

Based on our numerical results we have found out that for values of the ratio $U/W \geq 1/6$ there are serious differences in shapes of the one-particle spectrum calculated for the degenerate Hubbard hamiltonian in a non-self-consistent and a self-consistent way. The additional structure on the one-particle spectrum which can appear in a non-self-consistent approach, is always smoothed-out by the self-consistent process regardless of the shape of a starting LDOS (rectangular or fcc), a band filling and a strength of Coulomb correlations. For single-band Hubbard model the situation is somewhat different. For the rectangular uncorrelated LDOS there is no additional structure on the one-particle spectrum and the self-consistent process brings no significant effects. However, for the fcc starting LDOS a satellite peak can appear depending on the value of the band filling but it is removed by the self-consistent procedure. Hence, we conclude there is no

additional structure due to Coulomb correlations on the one-particle spectrum for the single-band or degenerate band Hubbard hamiltonian if the problem is treated in the self-consistent way for rectangular and fcc starting $D_0(E)$.

APPENDIX

The second-order part of the self-energy M(E) calculated at T = 0°K from Eq. (5) for the rectangular uncorrelated local density of states $D_0(E)$ (see Eq. (13)) reads (energy unit equals half an uncorrelated handwidth):

$$M(E) = \frac{U^2}{8} \sum_{i=1}^{8} (I_i(E) - I_{i+8}(E)), \qquad (A.1)$$

where

$$I_i(E) = \frac{1}{2}(E + A_i)^2(\ln|E + A_i| - \frac{1}{2}) + \frac{i\phi}{2}(A_i + E)^2 \qquad (A.2)$$

and

$$\begin{aligned}
&A_1 = E_F - 2, && A_9 = -A_8,\\
&A_2 = -E_F - 2, && A_{10} = -A_6,\\
&A_3 = A_2, && A_{11} = A_{10},\\
&A_4 = -E_F, && A_{12} = -1 - 2E_F,\\
&A_5 = 1 - 2E_F, && A_{13} = A_4,\\
&A_6 = 1, && A_{14} = 2 - E_F,\\
&A_7 = A_6, && A_{15} = A_{14},\\
&A_8 = 3, && A_{16} = -A_2,
\end{aligned} \qquad (A.3)$$

and

$$\begin{aligned}
&\phi = 0 \quad \text{for} \quad E + A_i > 0,\\
&\phi = \pi \quad \text{for} \quad E + A_i < 0,\\
&I_i = 0 \quad \text{for} \quad E + A_i = 0.
\end{aligned} \qquad (A.4)$$

We also give formula for the one-particle spectrum in the case of a rectangular uncorrelated LDOS (the non-self-consistent result) and $E_F = 0$ (the middle of the band):

$$D(E) = \frac{1}{8}\{\theta(-1 - E - \mathrm{Re}M(E)) - \theta(1 - E - \mathrm{Re}M(E)) +$$

$$+ \frac{1}{\pi}[\mathrm{arctg}\frac{-\mathrm{Im}M(E)}{E - 1 - \mathrm{Re}M(E)} - \mathrm{arctg}\frac{-\mathrm{Im}M(E)}{E + 1 - \mathrm{Re}M(E)}]\}, \qquad (A.5)$$

where M(E) is given in Eqs. (14), (15).

REFERENCES

1. Kisker E. - J.Phys.Chem., 1983, 87, p.3597.
2. Oh S.-J., Allen J.W., Mikkelsen J.C.,Jr. - Phys.Rev., 1982, B26, p.4845.
3. Penn D.R. - Phys.Rev.Lett., 1970, 42, p.921.
4. Liebsch A. - Phys.Rev., 1981, B23, p.5203.
5. Dietz R.E. et al. - Phys.Rev., 1981, B24, p.6820.
6. Kanski J., Nilsson P.O., Larsson C.G. - Solid State Comm., 1980, 35, p.397.
7. Treglia G., Ducastelle F., Spanjaard D. - J.Physique,1980, 41, p.281.
8. Treglia G., Ducastelle F., Spanjaard D. - J.Physique, 1982, 43, p.341.
9. Kleinman L., Mednick K. - Phys.Rev., 1981, B24, p.6880.
10. Kajzar F., Friedel J. - J. Physique, 1977, 39, p.397.

Received by Publishing Department
on July 16, 1987.

Таранко Р., Таранко Э., Малек И. E17-87-554

Самосогласованная теория корреляционных эффектов в переходных металлах

В модели Хаббарда в рамках самосогласованной теории возмущений во втором порядке по параметру разложения U/W (U- кулоновское взаимодействие, W - ширина зоны) рассмотрено влияние корреляционных эффектов на одночастичную плотность состояний в переходных металлах. Показано, что в самосогласованном расчете исчезает ранее предсказываемый дополнительный пик в плотности состояний.

Работа выполнена в Лаборатории теоретической физики.

Сообщение Объединенного института ядерных исследований. Дубна 1987

Taranko R., Taranko E., Malek J. E17-87-554

Self-Consistent Treatment of Coulomb Correlations in Transition Metals

Electron correlation effects in transition metals are studied within the Hubbard model by the self-consistent second-order-perturbation theory in U/W (U: Coulomb integral; W: bandwidth). It is shown that a satellite structure on one-particle spectrum predicted by the non-self-consistent second-order-perturbation theory disappears when the problem is treated in a self-consistent way.

The investigation has been performed at the Laboratory of Theoretical Physics, JINR.

Communication of the Joint Institute for Nuclear Research. Dubna 1987